Electronic-cluster model of yttrium iron garnets

R. J. Wojciechowski,* A. Lehmann-Szweykowska, and R. Micnas
Institute of Physics, Adam Mickiewicz University, ul. Umultowska 85, 61-614 Poznań, Poland

G. A. Gehring
Department of Physics and Astronomy, University of Sheffield, Sheffield S3 7RH, United Kingdom

P. E. Wigen
Department of Physics, Ohio State University, Columbus, Ohio, USA
(Received 22 December 2003; published 30 June 2004)

We review electronic and magnetic properties of yttrium iron garnets, considered as a superlattice of quantum dots of two different types. Those are the tetrahedral and octahedral iron-oxygen clusters characterized by their respective localized energy levels with the orbital eigenstates, specified by the clusters' respective point symmetries. We discuss two-dot mechanisms of the superexchange coupling between spins, attached to the orbital states, via the *p-d* tunneling, only (between clusters of different types), or via the *p-d* tunneling combined with the next-nearest neighbor *p-p* hopping (between clusters of the same type). The electronic density of states of a superlattice of the clusters is found and analyzed both for pure and valence-uncompensated garnet systems. A scheme of control of the superexchange coupling due to an external magnetic field, applied to the system is proposed.

DOI: 10.1103/PhysRevB.69.214434 PACS number(s): 73.22.−f, 75.50.Gg

I. INTRODUCTION

Interesting experimental data indicate that in yttrium iron garnets (YIG's) with valence-uncompensated doping, such as Ca:YIG, an application of the external magnetic field can significantly influence both the magnetic properties and the electric transport in the system.[1–3] The theoretical analysis presented in this paper is an attempt to propose a microscopic model, which could explain the empirical data in terms of the quantum dot approach. Quantum dots are generic systems for exploring the physics of small, coherent quantum structures. Valence-uncompensated doping on yttrium sites induces either excess electrons (e.g., Si:YIG), or compensating holes (e.g., Ca:YIG) in the system. Compensating holes and/or electrons, when located in quantum-confined structures such as iron-oxygen octahedrals and tetrahedrals, can influence the magnetic structure of the whole system. Moreover, they can be transported between different units. In our study, both the orbital and spin degrees of freedom are treated at the same footing. The crystal unit cell of YIG is built from 12 tetrahedral (FeO_4) and 8 octahedral (FeO_6) iron-oxygen *p-d* clusters.[4,5] In pure YIG the ground state ($L=0, S=\frac{5}{2}$) of Fe^{3+} has all five orbital states occupied by the electrons with mutually parallel spins. This specific situation indicates why a concept of compensating holes, induced by valence-uncompensated doping, can be useful in interpretation of the electronic structure of the derivatives of YIG. In the tetrahedral cluster, the central iron site is surrounded by the four oxygen nearest neighbors, whereas the octahedral cluster, apart from its central iron, consists of six anion sites. In the undoped system the O^{2-} ions have all their six orbital and spin states occupied. In the case of the oxygen ions again the concept of compensating holes seems to be easy to interpret. The point symmetry group of the tetrahedron is S_4, and that of the octahedron is S_6. The clusters of either type can be labeled by their respective central iron sites. The overall symmetry of the garnet is cubic and its space symmetry group is O_h^{10}. The *p-d* clusters of the same type are separated from one another, whereas the nearest-neighbor octahedron and tetrahedron share an oxygen corner. It also has to be mentioned that 12 sites of a third (dodecahedral) type are populated by three-valence yttrium ions with the closed electronic shells. Since an interpretation of the results concerning YIG, doped with calcium, is a priority in this paper, it seems to be more convenient to express an electronic structure of the system in terms of holes rather than in terms of the electrons. The argument is that all the available experimental information indicates that the electric conductivity in Ca:YIG is of the *p* type.

Thus, the system consists of holes of two types: the narrow-band 3*d* holes and 2*p* holes, which populate the anion eigenstates. The simplest possible Hamiltonian, which can be used as a point of departure to account for the magnetic and transport properties of YIG and its derivatives, is an extended three-band Hubbard model:[6,7]

$$\hat{H} = \hat{H}_{3d} + \hat{H}_{2p} + \hat{H}_{p\text{-}d} + \hat{H}_Z, \tag{1}$$

$$\hat{H}_{3d} = E_a \sum_{i,\alpha,m} \hat{n}_{i,\alpha,m} + D_a \sum_{i,\beta,m} \hat{n}_{i,\beta,m} + E_d \sum_{j,\beta,m} \hat{n}_{j,\beta,m} + D_d \sum_{j,\alpha,m} \hat{n}_{j,\alpha,m} + \frac{U}{2} \sum_{i,\sigma,m} \hat{n}_{i,\sigma,m}\hat{n}_{i,\sigma,-m}, \tag{2}$$

where

$$\hat{H}_{2p} = E_p \sum_{f,\sigma,m} \hat{n}_{f,\sigma,m} + \frac{1}{2} \sum_{f,f',\sigma,\sigma',m} t_{ff'}(\sigma,\sigma') \hat{c}^{\dagger}_{f,\sigma,m} \hat{c}_{f',\sigma',m} \tag{3}$$

and

$$\hat{H}_{p\text{-}d} = \sum_{i,f} V_{p\text{-}d}(i,f) \hat{d}^{\dagger}_{i} \hat{c}_{f} + \text{H.c.}, \tag{4}$$

where

$$\hat{n}_{i,\sigma,m} = \hat{d}^{\dagger}_{i,\sigma,m} \hat{d}_{i,\sigma,m}, \quad \hat{n}_{f,\sigma,m} = \hat{c}^{\dagger}_{f,\sigma,m} \hat{c}_{f,\sigma,m}. \tag{5}$$

The Hamiltonian $\hat{H}_{3d}$ describes the narrow-band 3*d* electron states, in the localized limit, with the strongest on-site Hubbard repulsion between the opposite-spin states $(m,-m)$ taken into account (the parameter U). Five orbital 3*d* states are separated into the t_{2g} triplet (β) and e_{eg} doublet (α) under the influence of the largest cubic contribution to the crystal field. The ground state of the 3*d* compensating hole in the tetrahedral position is the t_{2g} triplet (the energy E_d), and in the case of the octahedral site it is the e_g doublet (the energy E_a). The parameters D_d and D_a are the energy separation between the cubic energy levels at the tetrahedral and octahedral sites, respectively.

The indices i,j label the *a* and *d* iron sites, respectively. Of course, the summation over α, β, and σ in the Hubbard term runs over all the orbital states at all the iron sites. The second term of the Hamiltonian $(\hat{H}_{2p})$ concerns the 2*p* electron states. The 2*p* triplet t_{1u} at the oxygen sites is not split in the cubic crystal field. A possible direct intrasystem *p*-*p* hopping to the next-nearest neighbor (NNN) site[8] is considered, but the Hubbard on-site repulsion is neglected as small in comparison with that at the iron ions.

The third term of the Hamiltonian $(\hat{H}_{p\text{-}d})$, i.e., the 2*p*-3*d* tunneling between the oxygen and iron orbital states, accounts for a possible intersystem communication. $V_{p\text{-}d}(i,f)$ are two-site tunneling integrals. The indices i and f denote both the sites and the appropriate orbital and spin states localized at the sites. The Hamiltonian is extended by the standard Zeeman term $\hat{H}_Z$ [see Eq. (16)].

With an external magnetic field applied to the system we can control both its magnetic interactions and the electric transport.[9,10] Different orientations of the applied field with respect to the crystal axes can play a crucial role in the process due to the orbital contribution to the magnetic moment of the particles.

The on-site exchange (Hund) interaction is omitted in the Hamiltonian (1) for the following two reasons: first, what really matters most in our analysis is the Hubbard repulsion between carriers on the same orbital and opposite spin states at the same site since the symmetry enables us to specify precisely the single-hole orbital states. Second, the Hund term can be perturbatively included.[11] It determines an $S=5/2$ state of the 3*d* electrons and it is taken into account by assuming the Hund rule.

In order to apply the model to the YIG derivatives with electric conductivity of both *n* and *p* types, one should express the extended Hubbard model in terms of the 3*d* and 2*p* states, and in the specific case assume the right order of the cubic doublet (e_g) and triplet (t_{2g}) at the octahedral and tetrahedral iron sites. Of course, the relative energy positions of the 3*d* and 2*p* states, i.e., the parameters, E_d, E_a, and E_p, must be also changed accordingly.

In the first step of our procedure, this Hamiltonian is projected separately onto the tetrahedron and octahedron, neglecting both the *p*-*p* hopping and, also, the occurrence of the mutual oxygen corner between each pair of the nearest-neighbor (NN) tetrahedral and octahedral clusters. The group-theoretical analysis provides information on all the symmetry-permitted hybridizing 3*d* and 2*p* states,[8] which can then be used as proper initial states in the perturbation procedure, with the *p*-*d* tunneling term considered as a perturbation. Finally, a four-dimensional Hilbert subspace is obtained, whose basis consists of two 3*d* and 2*p* orbital states with nonzero matrix elements of the *p*-*d* hybridization between them, and two spin states attached to either of them.[12] In the next step, the intercluster *p*-*d* hybridization that results from the occurrence of the mutual oxygen corner of the nearest tetrahedral and octahedral clusters is taken into account together with the direct *p*-*p* hopping, which gives rise to the motion of the carrier.

Both types of the motion, i.e., that between clusters of the same symmetry, mediated by the *p*-*d* tunneling combined with the *p*-*p* hopping, as well as that between tetrahedral and octahedral clusters, mediated solely by the *p*-*d* hybridization, result in broadening of the single-hole energy levels, which are attached to each of the 20 iron-oxygen clusters of the crystal unit cell.

As might have been expected, the Hubbard on-site repulsive interaction between holes with the same orbital states and opposite spins finally results in the occurrence of the magnetic superexchange interactions between the clusters, and further it determines a type of the magnetic order of the whole system.

The problem of superexchange will be discussed, in great detail, for the orbital ground states in terms of the difference in energies, corresponding to the parallel (spin triplet) and antiparallel (spin singlet) mutual orientations of the spins, attached to the respective orbital ground states of the *p*-*d* clusters.[10] The outlined procedure serves also as a starting point in a calculation of the cluster electronic density of states.

The paper is organized as follows. In Sec. II, the energy levels and their respective eigenstates, labeled by the irreducible representations of the respective symmetry groups, are thoroughly discussed. Also, the question of the hole localization on either the iron or oxygen sites of the cluster is analyzed on the basis of the wave functions of the cluster's orbital eigenstates. In Sec. III, magnetic superexchange interactions between two clusters of different types are introduced and analyzed with special emphasis put on the question of spin factorization of the respective *p*-*d* and *p*-*p* transition matrices. The magnitude of the superexchange integral between the iron-oxygen clusters is analyzed as a function of the tunneling parameter. Moreover, the influence of an external magnetic field on the inter-cluster exchange mechanism

is studied,[13–15] which shows how the exchange coupling can be controlled experimentally. For valence-uncompensated doping, extra holes are induced, and consequently the exchange mechanisms need to be reanalyzed.

Section IV deals with a diagonalization of both the *p-d* and *p-p* spin-factorized transition matrices for the whole supercrystal unit cell consisting of 20 iron-oxygen clusters. Finally, the electronic density of states (EDOS) is obtained. Within the framework of the proposed quantum dot model, a connection between the model parameters and magnetic properties of the system is discussed with the indication for the antiferrimagnetic ground state, which is in agreement with the experimental results.

II. SINGLE-HOLE ENERGY LEVELS AND EIGENSTATES OF THE *p-d* QUANTUM DOTS

In the first step of the procedure described above, the truncated Hubbard Hamiltonian, is projected onto a single iron-oxygen cluster of either type. It turns out that, due to the presence of the on-site Coulomb repulsion, the matrix of the projected Hamiltonian is naturally factorized with respect to the spin. For clusters of both types, the orbital wave functions are assumed in the LCMO-like (linear combinations of molecular orbitals) form, i.e., as linear combinations of the single-particle $3d$ and $2p$ states, with their coefficients determined in a diagonalization procedure with the *p-d* tunneling as a perturbation. Within the framework of the group theory, we can precisely determine the original proper symmetry-permitted single-hole states.[8] For obvious physical reasons, those are linear combinations of these $3d$ and $2p$ states, which guarantee nonvanishing *p-d* tunneling. For the sake of further discussion, it seems to be important to remember that they must be eigenstates of these irreducible representations of the respective point symmetry groups, whose Cartesian product, if the point groups are extended to the space group of the crystal, can induce one of the transitive irreducible representations (irreps) of the space symmetry group O_h^{10}. For the octahedral cluster, all the Cartesian products are equal to the irreducible representation $a_u^{S_6}$. The cubic doublet $e_g^{O_h}$ is not actually split as the two irreps of the group S_6, which label the $3d$ wave functions obtained from the doublet, are mutually complex conjugate. Those are $e_g^{S_6}$ and $(e_g^{S_6})^*$, respectively. The cubic triplet $t_{2g}^{O_h}$ is split into a singlet, labeled by the irreducible representation $a_g^{S_6}$, and the doublet labeled again by $e_g^{S_6}$ and its complex conjugate. Eigenstates both at the iron center of the cluster and at each of its oxygen sites can be obtained by the well-known projection procedure. The eigenstate of all the octahedral oxygen sites $|P_a(\nu)\rangle$ is given by a linear combination of the single-hole ν states, where ν is $e_u^{S_6}$, $(e_u^{S_6})^*$, and $a_u^{S_6}$, respectively, at each site with half of the states having the opposite sign of their phase factors.

In the case of the tetrahedron, the ground-state cubic triplet t_{2g} is split into the $b_{3d}^{S_4}$ singlet and the doublet whose states are labeled by the complex representation $e_{3d}^{S_4}$ and its conjugate, respectively. The excited cubic doublet is split into the $a_{3d}^{S_4}$ and $b_{3d}^{S_4}$ singlets. The $2p$ t_{1u} triplet states are split into $b_{2p}^{S_4}$ singlet and the doublet, which corresponds to the irreducible representation $e_{2p}^{S_4}$ and its complex conjugate. Again, as in the case of the octahedron, both the $3d$ and $2p$ states are obtained by using the projection procedure. Likewise, the appropriate Cartesian products of the $3d$ and $2p$ states are equal either to the irreducible representation b^{S_4} or to the irreducible representation e^{S_4}. Analogous to the previous case, the oxygen wave function of each tetrahedron $|P_d\rangle$ is a linear combination of the four single-site $b_{2p}^{S_4}$, or $e_{2p}^{S_4}$ states with half of the sites having the opposite phase factor to that of the others.

After some simple algebra, from each 2×2 submatrix corresponding either to the spin $m(a)$ or $m'(d)$, two eigenenergies E_{1l} and E_{3l} $(l=a,d)$ are obtained with their respective eigenstates. The eigenenergies are given in the following form:

$$E_{1(3)}^{l} = 1/2(E_l + E_p) \mp 1/2\sqrt{(E_p - E_l)^2 + 4\gamma_l^2 V_{p\text{-}d}^2(l)}, \quad (6)$$

where both the on-site energies E_l as well as the coefficients γ_l are determined by the relevant irreducible representations of the symmetry group. In the same diagonalization procedure four corresponding eigenstates are determined with contributions of the appropriate $3d$ state determined by the coefficients $c_{1l}^{(1)}$ and $c_{1l}^{(3)}$, whereas the contributions of the oxygen states $|P\rangle_l$ are determined by $c_{3l}^{(1)}$ and $c_{3l}^{(3)}$ $(l=a,d)$, respectively. The coefficient can be also expressed in a standard simple form:

$$c_{1l}^{(1)} = c_{3l}^{(3)} = \cos(\lambda_l/2) \quad (7)$$

and

$$c_{3l}^{(1)} = -c_{1l}^{(3)} = \sin(\lambda_l/2), \quad (8)$$

where

$$\tan(\lambda_l) = 2\gamma_l^2 V_l^2/(E_l - E_p). \quad (9)$$

The second 2×2 submatrix of the Hamiltonian, which corresponds to the opposite value of the spin, i.e., $-m_s$ for an octahedral cluster (a) and $-m_s'$ for a tetrahedral cluster (d), also gives two eigenenergies for either cluster: E_{2l} and E_{4l} $(l=a,d)$:

$$E_{2(4)}^{l} = 1/2(E_l + U + E_p) \mp 1/2\sqrt{(U - E_p + E_l)^2 + 4\gamma_l^2 V_{p\text{-}d}^2(l)}. \quad (10)$$

Again, the $3d$ contribution to the eigenstates are determined by the coefficients, $c_{2l}^{(2)}$ and $c_{2l}^{(4)}$, whereas the $2p$ contributions are given by $c_{4l}^{(2)}$ and $c_{4l}^{(4)}$ for the clusters of both types:

$$c_{2l}^{(2)} = c_{4l}^{(4)} = \cos(\lambda_l/2) \quad (11)$$

and

$$c_{4l}^{(2)} = -c_{2l}^{(4)} = \sin(\lambda_l/2), \quad (12)$$

where

$$\tan(\lambda_l) = 2\gamma_l^2 V_l^2/(U + E_l - E_p). \quad (13)$$

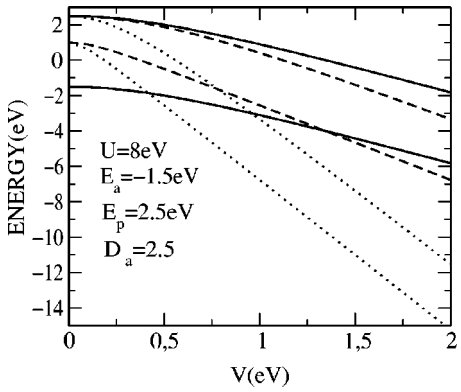

FIG. 1. The lowest-lying and first excited energy levels of the octahedral (a) cluster as a function of the p-d hybridization parameter, V. Solid lines show the orbital doublets, mutually conjugate linear combinations of $(e_g^{S_6})^*$ and $e_u^{S_6}$; dotted lines show the orbital singlets, linear combinations of $a_g^{S_6}$ and $a_u^{S_6}$; dashed lines show the orbital doublets, mutually conjugate linear combinations of $e_g^{S_6}$ and $e_u^{S_6}$. Values of the relevant model parameters are given inside the figure.

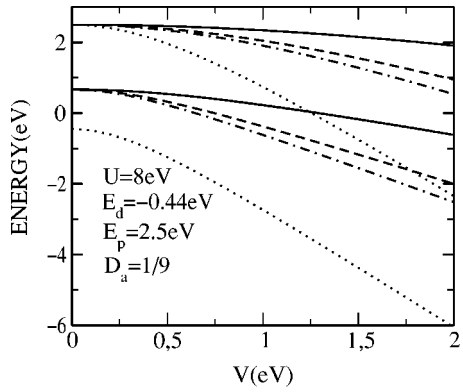

FIG. 2. The lowest-lying and first excited energy levels of the tetrahedral (d) cluster as a function of the p-d hybridization parameter, V. Dotted lines show the orbital sextet, all the mutually conjugate linear combinations of $b_{3d}^{S_4}$ with $e_{2p}^{S_4}$ and $e_{3d}^{S_4}$ with $e_{2p}^{S_4}$; dashed-dotted lines show the orbital singlets, linear combinations of $a_{3d}^{S_4}$ with $b_{2p}^{S_4}$; dashed lines show the orbital doublets, mutually conjugate linear combinations of $b_{3d}^{S_4}$ with $e_{2p}^{S_4}$; solid lines show the orbital doublets, mutually conjugate linear combinations of $a_{3d}^{S_4}$ with $e_{2p}^{S_4}$. Values of the model parameters are given inside the figure.

The eight energies are expressed in terms of the model parameters, which are the cubic crystal-field ground-state energies of the single-hole $3d$ localized at the octahedral (E_a) and tetrahedral (E_d) iron site, respectively. For certain representations, the ground-state energies must be shifted by the energy distance between the cubic doublet and triplet at the octahedral (D_a), and tetrahedral (D_d) iron sites, respectively. The on-site Coulomb repulsion parameter (U), energy of the $2p$ single hole localized at the oxygen site (E_p), and energy cost of the transfer between iron sites and their oxygen nearest neighbors, i.e., E_p-E_a and E_p-E_d, appear also in the formulas for the single-particle energies. Since we have decided to discuss the problem in terms of holes rather than electrons, we have e_g doublet as a ground state of the $3d$ holes on a octahedral iron site, and t_{2g} triplet on a tetrahedral. The energy level E_a is lower than E_d.

All possible two-site tunneling parameters are reduced to two basic ones, which are those between the $2p$ atomic states and the appropriate $3d$ (x^2,y^2,z^2) atomic states (V_a) and the appropriate $3d$ (xy,yz,zx) atomic states (V_d). The original basic tunneling parameters are then modified due to the broken symmetry of the p-d clusters.

In Fig. 1, all the lowest and first excited energy levels of the octahedral p-d cluster, corresponding to the possible Cartesian products of the $3d$ and $2p$ states, are presented as functions of the tunneling parameter. Among the lowest and first excited levels, there is one orbital singlet and two orbital doublets. As seen, in spite of the reduction of the overall cubic symmetry, the orbital doublet is still a ground state for a large range of the p-d tunneling. The doublet consists of two mutually conjugate linear combinations of the $e_g^{S_6}$ and $(e_u^{S_6})^*$ eigenstates. It is the only line in Fig. 1 that begins at the energy equal to E_a. The excited twin function (with opposite spin) is also indicated in the diagram. Like the other excited eigenstates, with $V=0$, its energy tends to E_p. For larger (and rather unrealistic) values of the tunneling parameter, there is a crossing of the ground energy levels, and the lowest-lying appears to be a singlet linear combination of the $a_g^{S_6}$ and $a_u^{S_6}$ eigenstates. The remaining orbital doublet consists of a linear combination of the irreducible representations $e_g^{S_6}$ and $e_u^{S_6}$, and their complex conjugates. This doublet, however, is expressed in terms of the original $t_{2g}^{O_h}$ cubic functions. Both the orbital singlet and the doublet at $V=0$, reach the point of E_a+D_a, i.e., that of the cubic triplet. The appropriate excited doublet (with opposite spin) is also presented in Fig. 1. The on-site repulsion parameter U, is fixed.

In Fig. 2, the lowest and first excited energy levels of the p-d tetrahedral cluster are presented as a function of the tunneling parameter. In this case, for the whole range of the tunneling parameter, a highly degenerate energy level is obtained as a ground state of the cluster. Those are actually three doublets, consisting of mutually conjugate functions, and their degeneracy is accidental. The first doublet is a linear combination of $e_{3d}^{S_4}$ with $e_{2p}^{S_4}$, and its complex conjugate; the second is $b_{3d}^{S_4}$ combined with $b_{2p}^{S_4}$, and the complex conjugate. The third doublet is represented by mutually conjugate linear combinations of $b_{3d}^{S_4}$ and $e_{2p}^{S_4}$. The energy of the three doublets originates at the energy E_d. The corresponding energy eigenlevel with the opposite spin is given in the diagram as well. The remaining energy levels, originating from the cubic doublet, i.e., at the point E_d+D_d, are the orbital singlet $(a_{3d}^{S_4},b_{2p}^{S_4})$ and two doublets $(a_{3d}^{S_4},e_{2p}^{S_4})$ and $(b_{3d}^{S_4},e_{2p}^{S_4})$ with their respective conjugate combinations. Again, all the opposite-spin energy levels begin at $E=E_p$.

In order to compare the a and d results with each other, in Fig. 3 two complete sets of the four energy eigenvalues, which include the respective ground states of the tetrahedral and octahedral clusters, are shown. For the tetrahedral cluster, each of the four energy levels correspond to its three orbital doublets, whereas for the octahedral cluster the eigenstates are the single orbital doublets. The energies are

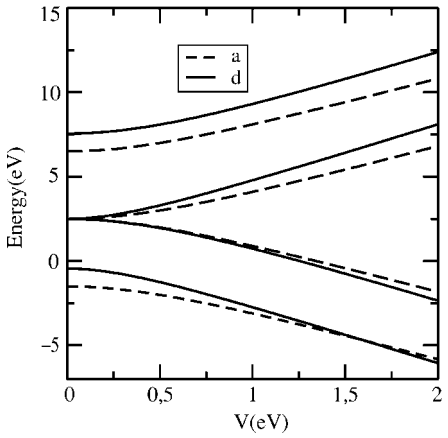

FIG. 3. All four energy levels of the sets with the respective ground states of the octahedral (dashed lines) and tetrahedral (solid lines) clusters, respectively, versus the *p-d* hybridization parameter, *V*. The remaining model parameters take the following values: $U=8$ eV, $E_a=-1.5$ eV, $E_d=-0.44$ eV, $E_p=2.5$ eV.

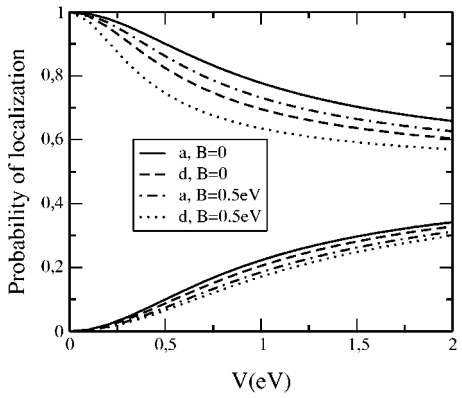

FIG. 4. Probability of localization at the iron sites for the lowest-lying and corresponding opposite-spin energy levels of the octahedral and tetrahedral clusters, respectively, vs the *p-d* hybridization parameter, *V*, with ($B=0.5$ eV) and without ($B=0$) the external magnetic field.

given as functions of the tunneling parameters. For the sake of simplicity, we assumed the tunneling parameters to be equal to each other, i.e., $V_a=V_d=V$. The Hubbard parameter, *U*, is fixed. The actual values of the microscopic parameters are the same as those given in Figs. 1 and 2.

Localization probabilities either at the iron, or at the surrounding oxygen sites, for different eigenstates of the same Hilbert subspace, are determined as modulo-squared coefficients of the appropriate contributions to the respective eigenfunctions. For instance, the localization probability at the iron site in the ground and its opposite-spin excited energy level are determined as follows:

$$P_{1l}^{Fe}=|c_{1l}^{1}|^2 \tag{14}$$

and

$$P_{2l}^{Fe}=|c_{2l}^{2}|^2, \tag{15}$$

where $l=a,d$. The probabilities are analyzed as functions of the tunneling parameter, *V*, and further, also, as those of a varying external magnetic field, since we believe that, by application of an external magnetic field, an external control of the system can be maintained. As might have been expected, for the lowest-lying eigenstate, the probability of localization at the iron site exceeds that at the surrounding oxygens. In the states with the spin orientation opposite to that of the ground energy level, there is a larger probability that the hole and/or electron gets localized at the surrounding oxygens. It holds for both types of clusters. In pure YIG, only the lowest of each set of the four energy levels is occupied, and the hole remains at the iron site. In calcium-doped YIG, for instance, a compensating hole, which must have its spin opposite to those of the holes already present at the cluster, will occupy the oxygens. However, there is a finite probability that it can get localized at the iron, forming a Fe^{4+}, which has been earlier suggested in the literature.

Let us now analyze the probability of the occupation of the iron sites in the lowest-lying and first excited eigenstates for both the octahedral and tetrahedral clusters with respect to the tunneling parameter, *V*, without as well as with an external magnetic field. The result can be changed by an application of the field, which has the tendency to lower the probability of localization at iron sites, increasing thereby a possibility of localization at the oxygens. We have decided not to display the occupation probabilities at the oxygen sites, since they represent a mirrorlike reflection of those for the iron, however, with the reversed order of the respective eigenstates. The probability of localization is bigger at an octahedral rather than at a tetrahedral iron site. It means that there is a possibility either of formation of a Fe^{4+} octahedral iron ion or the compensating hole will get localized at the oxygen sites hybridizing with the tetrahedral iron states. The results, used as an illustration in Fig. 4, correspond to the two lowest-lying eigenstates of each of the two *a* and *d* sets given earlier in Fig. 3.

From two possible contributions to the magnetic moment, the spin is already considered, by taking into account the Hubbard term in the Hamiltonian (2). This is an occurrence of the orbital contribution, which explains the splitting of the eigenenergy levels. The Hubbard Hamiltonian projected onto the *p-d* clusters is extended by the standard Zeeman term:

$$\hat{H}_Z=-\mu_B\vec{B}\cdot\sum_i(\hat{\vec{L}}_i+2\hat{\vec{S}}_i), \tag{16}$$

where $\hat{\vec{L}}_i$ and $\hat{\vec{S}}_i$ denote the orbital angular momentum and spin operators of the *p-d* cluster *i*, respectively. Both in the cases of the octahedron and tetrahedron, we restrict our discussion to the effect of the field applied along one of the principal axes of the bulk system, i.e., the $\langle 111\rangle$ axis, which is identical with the orientation of one of the main axes of the octahedron, but not of the tetrahedron.

The influence of the magnetic field on the four energy levels of the octahedral cluster (a), already given in Fig. 3, is presented graphically in Fig. 5. As the field gets stronger,

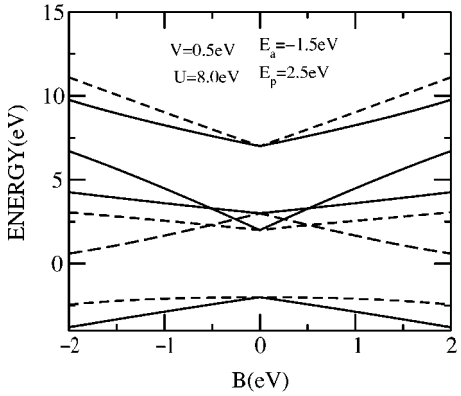

FIG. 5. Effect of the external magnetic field, applied along the ⟨111⟩ axis on the doublet eigenvalues of the octahedral cluster. The eigenstates are the same as those given in Fig. 3. The solid and dashed lines show both eigenenergies of each doublet. Values of the relevant model parameters are given inside the figure.

crossings of the middle-lying energy levels occur, which can imply both a flip of the spins attached to the appropriate orbital eigenstates and an appropriate change of the hole/electron localization.

As mentioned before, in the case of the tetrahedron, the orbital degeneracy of the ground energy level is much higher. It turns out that the field lifts completely the sixfold degeneracy. Three of the four sets of the resultant energies versus the applied field are presented in Fig. 6. Again, crossings of the middle-lying energy levels occur, suggesting a change of the spin orientation accompanied by the appropriate change of the localization. As follows from this discussion, the probability of localization in pure YIG is dominant at the iron sites, which means that the iron contribution also dominates in the *p-d* hybridized wave function, and, consequently, the high orbital degeneracy is only virtual. It becomes really important, however, when the system is doped and extra holes or electrons are introduced. Compensating particles occupy the opposite-spin hybridized eigenstates with larger probability of localization at the oxygen sites, and the higher orbital degeneracy.

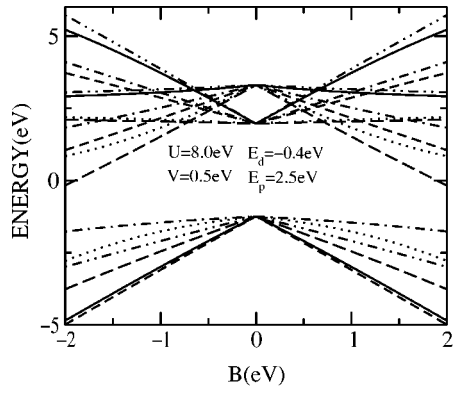

FIG. 6. Effect of the external magnetic field, applied along the ⟨111⟩ axis, on three of the set of the four eigenvalues of the tetrahedral cluster. The eigenstates are the same as those in Fig. 3. Values of the relevant model parameters are indicated inside the figure.

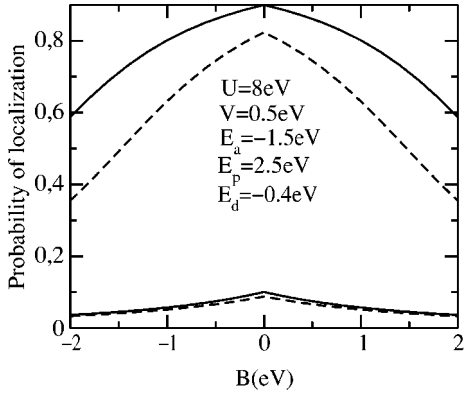

FIG. 7. Probability of localization at the iron sites for lowest-lying (the upper curves) and the corresponding opposite-spin (the lower curves) energy levels of the octahedral (the solid lines) and tetrahedral (the dashed lines) clusters, respectively, vs strength of the applied magnetic field. Again, values of the model parameters are given inside in the figure.

The probability of localization for the central iron sites, defined like that in Fig. 4, is shown as a function of the magnetic field for a selected fixed value of the tunneling parameter *V*, in Fig. 7. Again, the occupation probabilities for the oxygen sites do not need to be shown explicitly. With increasing strength of the field, the localization at the central iron sites decreases, which means that it gets larger at the oxygens. Thus, due to the applied field, there is a finite probability that the particle will be moved and its spin state alternated.

III. PAIRS OF THE OCTAHEDRAL AND TETRAHEDRAL *p-d* CLUSTERS

In order to get more insight into the electronic structure of the transition metal oxides of this specific type, within the framework of the cluster model,[15,16] let us start the analysis with a mixed pair of the *p-d* clusters. For the sake of simplicity, each cluster is considered as a quantum dot with a selected set of the four orbital states, attached to it, forming a basis of its Hilbert orbital subspace. As mentioned before, each pair of the nearest clusters belonging to the different sublattices share a common oxygen site that enables their mutual communication via the *p-d* tunneling only. The selection of the cluster orbital states for further discussion has been done on the basis of magnitude of the *p-d* tunneling matrix elements between the *a* and *d* clusters as well as on their response to the magnetic field. The diagonalization of the projected *p-d* tunneling Hamiltonian is performed for these selected sets of the respective single-hole eigenstates. Two cases need to be considered:

(i) The clusters have the same spin orientation in their respective ground states (ferromagnetic order or spin triplet).

(ii) The clusters have opposite spins in their respective ground states (antiferromagnetic order or spin singlet).

In each case, different off-diagonal transition matrix elements of the *p-d* Hamiltonian are obtained. As an example, two of the possible 16 matrix elements are presented below in an explicit form:

(i) for ferromagnetic order

$$A_{13}^{ad} = (A_{31}^{da})^* = c_{1a}^{(1)} c_{3d}^{(3)} \alpha V_a + \sqrt{2} c_{3a}^{(1)} c_{1d}^{(3)} \alpha^* V_d, \qquad (17)$$

(i) for antiferromagnetic order

$$A_{12}^{ad} = (A_{21}^{da})^* = c_{1a}^{(1)} c_{4d}^{(2)} \alpha V_a + \sqrt{2} c_{3a}^{(1)} c_{2d}^{(2)} \alpha^* V_d. \qquad (18)$$

The coefficient α can be expressed as follows:

$$\alpha = (1/4)(1 + \sqrt{3})(-1 + i). \qquad (19)$$

After some simple algebra, two different sets of the two-cluster single-particle energy levels with their respective eigenstates are found. Within the framework of this approach, pure YIG differs from its derivatives in the number of holes per quantum dot. In pure YIG, the population is one hole per cluster, which means that two of eight two-cluster energy levels are occupied. The total ground-state energy of the two-cluster system is therefore a sum of the two lowest-lying single-hole energy levels. As might have been expected,[10,11] in pure YIG, the spin-singlet ground-state energy level lies below the spin-triplet one for a wide range of values of the tunneling parameter, V, which means that a pair consisting of the octahedral and tetrahedral clusters favors mutually opposite directions of spins in their respective orbital ground states. Thus, the ground state of the two clusters must be a spin singlet ($S=0$). Information on the difference between the ferromagnetic and antiferromagnetic two-cluster energy D_{ad} enables us to estimate superexchange integrals at $T=0$ K as functions of the microscopic model parameters.[17–19] The conclusion is based on a well-known supposition that in the absence of the external magnetic field, this energy difference is simply equal to the superexchange integral J_{ad} between two spins $S=1/2$, attached to the orbital ground states of the clusters:

$$J_{ad} = E_f - E_{af}, \qquad (20)$$

where E_f and E_{af} stand for the ferromagnetic and antiferromagnetic energies of the two-cluster system, respectively. The results in Fig. 8 show the superexchange integral J_{ad} for pure (the solid line) and doped (the dotted line) system as a function of the p-d hybridization parameter V. With the magnetic field applied to the system, the spin triplet-singlet energy difference as a function of V is presented for pure (the dashed line) and doped (the dashed-dotted line) systems. The Hubbard repulsion parameter is fixed. In Fig. 9, the spin triplet-singlet difference in energy D_{ad} is given as a function of the applied magnetic field, for a fixed value of the hybridization parameter, and with the same, as previously, values of $U=8$ eV, $E_a=-1.5$ eV, $E_d=-0.44$ eV, and $E_p=2.5$ eV.

In the undoped system the superexchange integral J_{ad} is positive, as expected, with the external magnetic field equal to zero. The corresponding triplet-singlet energy difference D_{ad} changes its sign, however, at some finite magnetic field, and on the whole, it displays a particularly complex V dependence resulting from possible crossings of the second and third energy levels of the both clusters (cf. Figs. 5 and 6). To obtain the result with a weaker external magnetic field we should take into account the molecular field.

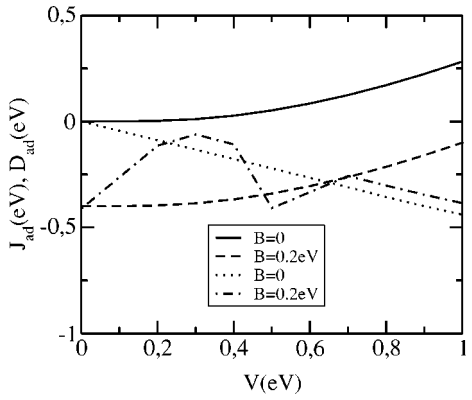

FIG. 8. The superexchange integral J_{ad} between spins attached to the ground orbital eigenstates of the a and d clusters vs the hybridization parameter V, without the external magnetic field B, for pure (the solid line) and doped (the dotted curve) system. And, the spin triplet-singlet energy difference D_{ad} with the external magnetic field $B=0.2$ eV again for pure (the dashed curve) and doped (the dotted-dashed curve) system. The relevant model parameters take the following values: $U=8$ eV, $E_a=-1.5$ eV, $E_d=-0.44$ eV, and $E_p=2.5$ eV.

Valence-uncompensated doping induces extra holes or extra electrons in the system. Within the framework of this model in Ca:YIG the third relevant hole is located at the same pair of two hybridizing clusters, so the third of the set of the eight eigenstates of the pair must be occupied. And, using Eq. (8), with the energies defined as sums of the three lowest-lying single-hole energy levels, we obtain the superexchange coupling integral between the pair of the spins, attached to the respective orbital ground states of the clusters. It turns out (Fig. 8) that rather parallel than antiparallel mutual orientation of the spins in the orbital ground states is favored, which means that an extra hole can change the sign of the superexchange interaction. Magnetic properties of the system are then influenced in two ways: not only directly by reducing the resultant spin, but also by changing the magnetic interactions.

In our analysis, an influence of the strong molecular magnetic field is omitted so our conclusions concerning the ex-

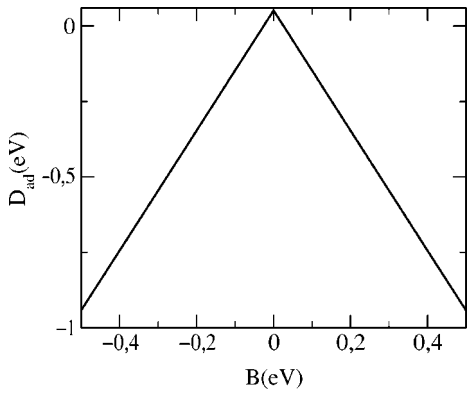

FIG. 9. The spin triplet-singlet difference in energy D_{ad} vs the applied magnetic field for an undoped system. Values of the relevant model parameters are $U=8$ eV, $E_a=-1.5$ eV, $E_d=-0.44$ eV, and $E_p=2.5$ eV.

ternal magnetic field effects can provide only a gross qualitative result.

Within the framework of the present approach, the superexchange interaction Hamiltonian consists of the contributions, corresponding to the interactions between particular pairs of spins. It can be expressed in the following simple form:

$$\hat{H}_{ex} = \sum_{\alpha\beta} J(\alpha,\beta)\vec{S}_{\alpha}\cdot\vec{S}_{\beta}, \tag{21}$$

where the summation runs over all the relevant orbital eigenstates of the respective quantum dots, and $\vec{S}_{\alpha(\beta)}$ denote the $S=1/2$ spins attached to the orbital states. Therefore, what we estimate from Eq. (8) is the particular contribution to the interaction, i.e., the integral $J(\alpha,\beta)$ with α and β being the ground orbital eigenstates of the respective clusters.

The problem becomes more complicated for two hybridizing clusters of the same type. The octahedral clusters share no oxygen sites. And the same is true about the tetrahedral clusters. Therefore a possible intrasublattice communication, involving clusters of one type, may occur via a combination of the *p-d* with *p-p* tunneling. Some simple space-symmetry analysis clearly proves that only the direct *p-p* hopping to the next-nearest oxygen neighbors is important as it brings the hole to the nearest cluster of the same sublattice.[4] And, it is the case for both types of the clusters. The direct *p-p* tunneling Hamiltonian is projected onto a space of the eight hybridized eigenstates of two clusters of the same type. Again, like in the previous case one has to consider the spin degrees of freedom. Two cases are distinguished from each other:

(i) Both clusters have same spins attached to their respective ground energy levels (ferromagnetic order or spin triplet).

(ii) The clusters have spins of the mutually opposite orientation attached to their ground energy levels (antiferromagnetic order or spin singlet).

In either case, a different set of off-diagonal matrix elements corresponding to possible transitions between the clusters is obtained. Since no spin-orbit coupling is considered, every transition between the clusters occurs with spin conservation.

As an example, both for the *a-a* and *d-d* pair, two of the 16 possible off-diagonal matrix elements of the tunneling Hamiltonian are given below in an explicit form:

(i) ferromagnetic order (spin triplet)

$$A_{13}^{aa(dd)} = \beta_{a(d)} c_{3a(d)}^{(1)} c_{3a(d)}^{(3)}, \tag{22}$$

(ii) antiferromagnetic order (spin singlet)

$$A_{12}^{aa(dd)} = \beta_{a(d)} c_{3a(d)}^{(1)} c_{4a(d)}^{(2)}, \tag{23}$$

where

$$\beta_a = 2\beta_d = 1/2t_2. \tag{24}$$

It is reflected in the formulas that transitions between the hybridizing clusters result from the direct *p-p* tunneling between the oxygen sites that are mutual second neighbors, and thus t_2 is the NNN tunneling integral between the $2p$ atomic states. The coefficients $c_{a(d)}$'s determine the oxygen contribution to the respective hybridized $3d-2p$ single-particle cluster state. The numerical coefficients in β are found in the group-theoretical projection procedure.[4]

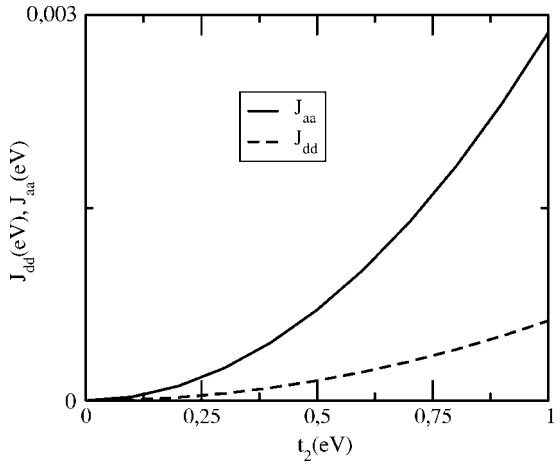

FIG. 10. The exchange integrals J_{aa} (the solid line) and J_{dd} (the dashed line) between spins, attached to the orbital ground states of the NN octahedral and tetrahedral clusters, respectively, vs the *p-p* tunneling parameter t_2, for the pure system and without the external magnetic field. Values of the system parameters: $U=8$ eV, $E_a=-1.5$ eV, $E_d=-0.44$ eV, $E_p=2.5$ eV.

As before, in the case of the mixed pair of the *a* and *d* clusters, both pure YIG (Ref. 16) and its derivatives obtained by valence-uncompensated doping are discussed. Again, with respect to pure YIG, they differ in a number of the holes and/or electrons per cluster. The superexchange integrals J_{aa} and J_{dd}, respectively, are found from Eq. (20) with appropriately defined ground-state energy levels. For the same range of the microscopic parameters, values for the exchange integrals are much smaller than those obtained for the magnetic interaction between mixed, i.e., tetrahedral-octahedral pairs. And, they clearly indicate that the antiparallel mutual orientation of the ground-state spins is favored. The numerical results are shown in Figs. 10 (for the pure system) and 11 (the doped system). The superexchange integrals J_{aa} and J_{dd} are presented as functions of the *p-p* NNN tunneling parameter, t_2, with the fixed values of the Hubbard parameter, U, and the *p-d* hybridization parameter V.

Again valence-uncompensated doping changes the sign of the magnetic interactions in favor of the mutual parallel orientation of the relevant spins. All the estimations of the superexchange interactions in YIG, such as a comparison of inelastic neutron scattering data with the spin-wave spectra (see Ref. 15 for detail) remain in mutual agreement with respect to the sign and magnitude of the intersublattice superexchange interaction. In almost all of the well-known papers on YIG, the same value of J_{ad} is found (see: Refs. 16 and 17 and the references therein). Within the framework of the model proposed here, the inter-sublattice interaction is the only one whose origin is consistent with that of the Anderson superexchange. With respect to the actual magnitude of J_{ad}, however, it seems rather obvious that we derive

only one contribution to the resultant exchange parameter between the two *p*-*d* clusters [Eq. (20)], versus the total one, which is estimated from the spin-wave spectra. In this model, the intrasublattice magnetic interactions are mediated both by the *p*-*d* hybridization and by the NNN *p*-*p* tunneling. In spite of its alternating-spin origin, in the pure system the interactions favor the antiparallel spin orientation, and their respective magnitude is much smaller than that of the intersublattice interaction, which also remains in agreement with the results obtained from the experimental data.

IV. THE ELECTRONIC DENSITY OF STATES OF THE SUPERLATTICE

Within the framework of the present approach, the crystal of YIG can be regarded as a cubic superlattice of octahedral and tetrahedral quantum dots with a set of the specific orbital and spin eigenstates attached to each of them, forming its Hilbert space. Thus a crystal unit cell of YIG consists of 8 octahedral and 12 tetrahedral inequivalent quantum dots. They can be labeled by their respective central iron ions. The simplest way of estimating their size is a comparison of the iron $a(d)$-to-oxygen distance with half of the lattice constant $(a/2)$. As the iron-oxygen distances are almost identical, the ratio is approximately of the same order, i.e., 6 per a quantum dot.

Communication between the nearest quantum dots of the same type is mediated by the *p*-*d* hybridization combined with next-neighbor *p*-*p* hopping, whereas the intersublattice transfer can be mediated solely by the *p*-*d* hybridization because of the common oxygen site the *a* and *d* clusters share with each other. It is interesting that as the simple space-symmetry analysis shows, with respect to the *p*-*p* hopping, 8 octahedral quantum dots split spontaneously into four one-dimensional chains along the threefold crystal axes $\langle 111 \rangle$.[8] The reason is that the space symmetry permits each octahedral cluster to exchange holes and/or electrons with only two of its six nearest neighbors. It suggests also an occurrence of the strong anisotropy, both of the transport and magnetic properties. In the case of the clusters of the tetrahedral type no such restrictions are imposed by symmetry.

In order to find the electronic density of states we have to diagonalize the spatial Fourier transform of the Hubbard Hamiltonian (1) projected onto the crystal unit cell of YIG with a set of the single-hole eigenstates attached to each of the hybridizing clusters. The off-diagonal matrix elements can only be determined after having assumed a mutual spin orientation in all the clusters.

For the sake of clarity, this procedure can be considerably simplified by considering only a contribution to the electronic density of states, coming from the orbital ground state of each cluster. It means that each quantum dot is characterized by its four-dimensional spin-orbital Hilbert space, and, of course by its position in the crystal unit cell. There is an additional argument for considering only this specific contribution to the density of states. The first excited energy level lies above the Fermi level and plays a crucial role in the charge and spin transport.

As mentioned above, in the case of pure YIG one hole per quantum dot is assumed. It means that 20 eigenstates are occupied and the Fermi level is identical with the highest of them. Within the framework of this approach, different valence-uncompensated derivatives of YIG differ from one another in the number of electrons or holes per quantum dot. The extra holes in the Ca-doped system gives rise to a shift of the Fermi level to the right toward higher energies.

In the real crystal, 5 electrons are located at each cluster; however, we focus our attention on the one playing a crucial role in the determination of the magnetic and electric properties of the crystal. Consequently a diagonalization of the 80×80 Hamiltonian matrix must be performed. All the diagonal matrix elements are simply equal to one of the appropriate four eigenenergies of the iron-oxygen clusters [see Eqs (5) and (6)]. The off-diagonal matrix elements take the following form:

$$H(\vec{q})_{i,k} = f(\vec{q})_{i,k} \exp(i\vec{q} \cdot \vec{r}_{i,k}), \tag{25}$$

where $\vec{r}_{i,k} = \vec{r}_i - \vec{r}_k$ and both $\vec{r}_i$ and $\vec{r}_k$ are the position vectors of the iron ions in the superlattice unit cell. The indices *i* and *k* in the formula denote also the appropriate orbital states of the clusters.

The off-diagonal matrix elements fall into two categories: if *i* and *k* denote the clusters of different symmetry, i.e., *a* and *d*, respectively, then the matrix element $f_{i,k}$ is determined by the *p*-*d* hybridization. Its specific form depends upon the orbital eigenstates of the respective clusters [cf. Eqs. (16) and (17)]. If the matrix element is between the clusters of the same type, then the function $f(\vec{q})_{i,k}$ results from the NNN *p*-*p* tunneling. Again, its specific form is dependent on the orbital states [see Eqs. (21) and (22)]. The off-diagonal matrix elements are nonzero provided that the spins attached to the respective orbital states are equal to each other. It means that the final form of the Hamiltonian can only be found if a mutual magnetic orientation of the quantum dots is assumed. Since we analyze also an influence of the external magnetic field, it seems to be sensible to select just the two magnetic structures.[20,21] Those are collinear ferromagnetic order of all spins attached to the orbital ground states of the clusters, and collinear antiferrimagnetic order in which all spins of the clusters of one type are aligned in one direction and opposite to those of the clusters of the other type. In either case, a different form of the projected Hamiltonian is obtained.

The electronic density of states $D(E)$ can be expressed as follows:

$$D(E) = \sum_{E_i} A_i \, \delta(E - E_i), \tag{26}$$

where the summation in the formula runs over all the eigenvalues of the projected Hamiltonian (E_i). For each contribution to the density of states, the summation is also performed over the wave vector $\vec{q}$ along the $(\Gamma X R \Gamma)$ loop in the simple cubic Brillouin zone, i.e., from $\Gamma = (0,0,0)$ to $X = (0,\pi,0)$, farther to $R = (\pi,\pi,\pi)$ and finally back to the point of departure. The density of states is analyzed with respect to microscopic model parameters. Numerical results are shown in Figs. 12 and 13, where the curves represent EDOS both for

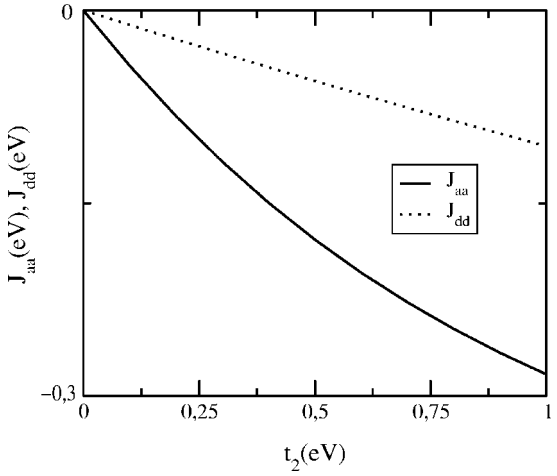

FIG. 11. The exchange integrals J_{aa} (the solid line) and J_{dd} (the dotted line) between spins attached to the orbital ground states of the NN tetrahedral clusters, respectively, vs the *p-p* tunneling parameter t_2, in the doped-system, without the magnetic field. Values of the microscopic parameters are like those in Fig. 10.

ferro- and antiferromagnetic mutual orientation of the ground-state spins of the *a* and *d* quantum dots. The effect depends upon the external magnetic field applied to the system (Fig. 13). The specific orientation of the external magnetic field, i.e., along the ⟨111⟩ axis, serves merely as an illustration. The problem was studied on a broader scale, showing that the system is anisotropic, which may be explained as a result of the orbital contribution to the magnetic moment of each quantum dot [see Eq. (15)].

V. CONCLUSIONS

In conclusion we have proposed and analyzed a microscopic model of yttrium iron garnets with excess holes or electrons, induced to the system, by valence-uncompensated doping. The system is considered as a superlattice consisting of two types of the *p-d* quantum dots with different sets of the localized eigenvalues and their respective orbital eigenstates. Both the energies of the octahedral and tetrahedral dots as well as localization of the holes and/or electrons either at the central iron or the surrounding oxygen sites can be controlled by an application of the external magnetic field. The magnetic moment of each quantum dot consists of the spin and orbital contributions and the external control of the situation can be maintained due to the standard Zeeman term.

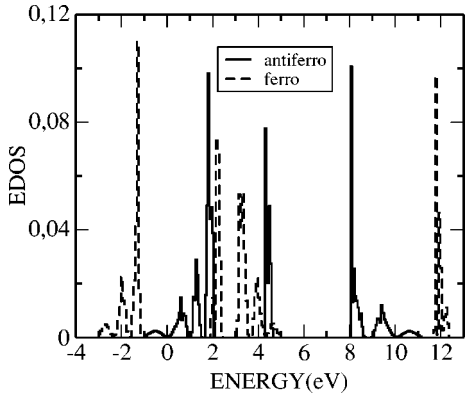

FIG. 12. The EDOS of YIG with an antiferromagnetic (the dashed line) and ferromagnetic (the solid line) mutual orientation of the ground-state spins of the nearest-neighbor *a* and *d* clusters, for $V=0.5$ eV, $t_2=0.25$ eV.

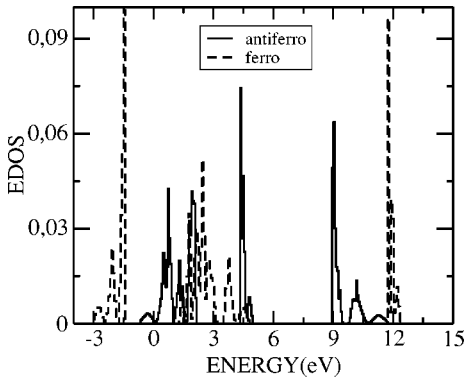

FIG. 13. The EDOS of YIG with mutually antiparallel (dashed line) and parallel (solid line) spins of the orbital ground states of the *a* and *d* clusters in the external magnetic field ($B=0.5$ eV and the same values of V and t_2 like those in Fig. 12).

Mutual communication between the dots of different types occurs via the *p-d* hybridization, whereas the transfer of the holes and/or electrons between the homogeneous dots is mediated by the *p-d* hybridization combined with the *p-p* tunneling to the next-nearest oxygen neighbors. The superexchange interaction between spins attached to the ground orbital states of the different clusters, estimated as a difference in the spin triplet and singlet energies, turns out to be antiferromagnetic, i.e., it favors antiparallel mutual orientation of the spins. The most remarkable feature of the coupling, however, is the change of its sign, which occurs at some finite value of the external magnetic field. The exchange coupling between spins, attached to the ground orbital eigenstates of the homogeneous dots, estimated in the same way, is mediated by the *p-d* hybridization combined with the *p-p* tunneling. It turns out to be antiferromagnetic as well, which is compatible with the empirical data. The ratios of the intra- and intersublattice interactions remain in agreement with the experimental results.

Within the framework of this model, the electronic density of states is also found. It is characterized by the sharp peaks corresponding to the eigenstates of the crystal unit cell, consisting of 40 quantum dots. The spins of the quantum dots can be controlled through their orbital degrees of freedom, by an application of the external magnetic field.

ACKNOWLEDGMENTS

R.J.W., A.L.S., and R.M. gratefully acknowledge partial support under the Grant No. PBZ-KBN-044/PO3/2001. R.M. also acknowledges support from the Foundation of Polish Science.

*Electronic address: wojrysz@main.amu.edu.pl

[1] G. B. Turpin, Y. J. Song, and P. E. Wigen, IEEE Trans. Magn. **31**, 3835 (1995).
[2] Y. J. Song, G. B. Turpin, R. E. Bornfreund, h. Aoyama, and P. E. Wigen, J. Magn. Magn. Mater. **154**, 37 (1996).
[3] P. E. Wigen. and Donglai (private communication).
[4] H. Donnenberg, S. Toebben, and A. Birkholz, J. Phys.: Condens. Matter **9**, 6359 (1997).
[5] S. Ishihara, J. Inoue, and S. Maekawa, Phys. Rev. B **55**, 8280 (1997).
[6] S. Robaszkiewicz, R. Micnas, and J. Ranninger, Phys. Rev. B **36**, 180 (1987).
[7] J. Zaanen and A. M. Oleś, Phys. Rev. B **37**, 9423 (1988).
[8] A. Lehmann-Szweykowska, T. Lulek, and M. M. Kaczmarek, J. Phys.: Condens. Matter **13**, 3607 (2001).
[9] C. Srinitiwarawong and G. A. Gehring, J. Phys.: Condens. Matter **13**, 7987 (2001).
[10] P. Recher, D. Loss, and J. Levy, cond-mat/0009270.
[11] F. D. M. Haldane and P. W. Anderson, Phys. Rev. B **13**, 2553 (1976).
[12] A. Lehmann-Szweykowska, R. J. Wojciechowski, and G. A. Gehring, Acta Phys. Pol. A **97**, 563 (2000).
[13] R. J. Wojciechowski, A. Lehmann-Szweykowska, J. Barnaś, and P. E. Wigen, NATO Science Series, II Mathematics, Physics and Chemistry, edited by A. Graja, B. R. Bułka, and F. Kajzar (Kluver Academic, 2002), Vol. 59, 297.
[14] R. J. Wojciechowski, A. Lehmann-Szweykowska, P. E. Wigen, and J. Barnaś, Phys. Status Solidi B **196**, 189 (2003).
[15] Eiichi Hanamura, Nguyen Trung Dan, and Yukito Tanabe, J. Phys.: Condens. Matter **12**, L345 (2001).
[16] F. Walz, J. H. V. J. Brabers, L. Torres, and H. Kronmüller, Phys. Status Solidi B **228**, 717 (2001).
[17] V. Cherepanov, I. Kolokov, and V. L'vov, Phys. Rep. **229**, 81 (1993).
[18] J. S. Plant, J. Phys.: Condens. Matter **10**, 4805 (1997).
[19] Th. Bruckel, W. Prandt, and P. Convert, J. Phys. C **20** 2565 (1987).
[20] H. Donnenberg and C. R. A. Catlow, Phys. Rev. B **50**, 744 (1994).
[21] A. Koper, A. Lehmann-Szweykowska, R. Wojciechowski, and M. Mucha, J. Phys.: Condens. Matter **7**, 1391 (1995).